The effect of temperature and strain rate on the interaction between an edge dislocation and an interstitial dislocation loop in α-iron

2007 J. Phys.: Condens. Matter 19 456211

(http://iopscience.iop.org/0953-8984/19/45/456211)

IOP PUBLISHING JOURNAL OF PHYSICS: CONDENSED MATTER

J. Phys.: Condens. Matter **19** (2007) 456211 (13pp) doi:10.1088/0953-8984/19/45/456211

The effect of temperature and strain rate on the interaction between an edge dislocation and an interstitial dislocation loop in α-iron

D Terentyev[1,4], L Malerba[1], D J Bacon[2] and Yu N Osetsky[3]

[1] Structural Materials, Institute of Nuclear Materials Science SCK-CEN, Boeretang 200, B-2400 Mol, Belgium
[2] Materials Science and Engineering, Department of Engineering, The University of Liverpool, Brownlow Hill, Liverpool L69 3GH, UK
[3] Computer Sciences and Mathematics, ORNL, Oak Ridge, TN 37831, USA

E-mail: dterenty@sckcen.be

Received 28 June 2007, in final form 16 August 2007
Published 15 October 2007
Online at stacks.iop.org/JPhysCM/19/456211

Abstract

The influence of temperature, T, and strain rate, $\dot{\varepsilon}$, on the reaction between the $\frac{1}{2}[111](1\bar{1}0)$ edge dislocation line and a periodic row of 4 nm interstitial dislocation loops with Burgers vector $\boldsymbol{b} = \frac{1}{2}[1\bar{1}1]$ in α-Fe has been investigated by means of molecular dynamics, using a potential developed recently for body centred cubic Fe (Ackland *et al* 2004 *J. Phys.: Condens. Matter* **16** 1). A dislocation segment with $\boldsymbol{b} = [010]$ is formed by favourable reaction in all cases: it is sessile in the $(1\bar{1}0)$ glide plane and leads to the formation of a screw dipole on the line under increasing stress. The mechanism controlling line breakaway and the corresponding critical stress depend mainly on T rather than $\dot{\varepsilon}$. At high T (300 and 600 K here) the length of the screw dipole is short ($<10b$) and the controlling mechanism is the glide of the [010] segment over the loop surface coupled with cross-slip of the short screws. The loop is totally absorbed on the line by transformation of $\boldsymbol{b}$ to $\frac{1}{2}[111]$. At low T, where thermal effects are negligible, a long ($\sim 100b$) screw dipole is drawn out and the controlling mechanism is annihilation of the dipole by screw cross-slip. This results in only partial absorption of the loop. By comparing the results with earlier ones obtained using an older interatomic potential, conclusions are drawn on the effects of interaction between edge dislocations and interstitial loops in iron.

(Some figures in this article are in colour only in the electronic version)

[4] Author to whom any correspondence should be addressed.

1. Introduction

Ferritic steels are major structural materials for current nuclear power plants and ferritic and/or ferritic/martensitic steels are prime candidate structural components in designs for future systems [1]. The exposure of these materials to neutron irradiation causes nanoscale damage that changes their properties. Depending on the temperature, alloy composition and neutron fluence, defects such as voids, gas bubbles, precipitates and dislocation loops can nucleate and evolve in the radiation damage, and can be sufficiently large to be observed by TEM in the microstructure of ferritic alloys after neutron irradiation. The presence of these defects can impede dislocation motion, thereby causing hardening and loss of ductility. Thus, understanding the mechanisms involved and gaining ability to predict their effects are important for assessment of lifetime and operational safety of materials exposed to neuron irradiation.

It is widely accepted that a multi-scale modelling approach provides a practical framework for tackling this problem. It begins with the production of atomic-scale defects in individual displacement cascades and ends with plasticity and fracture mechanics treatment of whole components, wherein the response of the material to changes in temperature and/or applied stress is of concern [2]. Methods of modelling dislocations under stress at the atomic and continuum levels lie between these extremes. The latter, known as dislocation dynamics (DD), can treat many dislocations and so links discrete defect behaviour to fracture mechanism models. DD requires specific information on dislocation mobility and mechanisms involved in reactions between dislocations and irradiation-induced defects, and this can be provided by atomic-scale computer simulations using molecular dynamics (MD). Such simulations have already demonstrated cases where elasticity theory is valid and also where its predictive capability breaks down due to the occurrence of unforeseen atomic mechanisms, e.g. [3, 4]. The latter situation has been found to arise even in molecular statics (MS) modelling for 0 K, where simulations most closely mimic the elasticity approximation [4, 5].

In the important case of α-iron, MS and MD have been used to investigate the interaction of an edge dislocation under applied stress with copper precipitates and voids and dislocation loops formed by self-interstitial atoms (SIAs), e.g. in [3, 6–8]. Less attention has been given so far to the screw dislocation [9, 10]. A comprehensive study of dislocation–loop interaction in iron was presented in [7, 8], where interactions between an edge dislocation and a row of hexagonal SIA loops, both with Burgers vector $\boldsymbol{b} = \frac{1}{2}\langle 111\rangle$, were considered. Simulations have shown that such loops, which are glissile and consist of an array of closely packed, parallel $\langle 111\rangle$ crowdions, are very mobile [11]. When their Burgers vector lies parallel to the $\{1\bar{1}0\}$ glide plane of the dislocation, they can be dragged by it at speeds that are a sizable fraction of the speed of sound [8]. When their $\boldsymbol{b}$ is inclined to the glide plane, they can be attracted by the gliding dislocation and react with it by moving to intersect the glide plane [7]. The defect arrangement created by the reaction and the maximum stress required for continued dislocation glide depend on temperature, applied strain rate and loop size. Loops containing either 37 or 331 SIAs in crystals deformed at strain rates from 2×10^6 up to 10^8 s^{-1} and temperatures from 0 to 450 K were modelled in [7]. Small loops are readily transformed by the reaction so that their $\boldsymbol{b}$ becomes the same as that of the edge dislocation line and they are simply absorbed on it as a pair of superjogs. Large loops react so that one side forms a segment on the line with $\boldsymbol{b}$ of $\langle 100\rangle$ type. The same reaction was found earlier for a 99-interstitial loop in [6]. At 100 K, the dislocation breaks away from this segment and leaves the original loop behind, whereas at 300 K and higher, the loop eventually transforms to form a pair of superjogs. In both cases, the large loop presents a strong obstacle to dislocation glide and the dislocation side-arms joined to the loop are pulled into screw orientation at the critical (maximum) stress. The critical stress was found to decrease only slightly with decreasing strain rate and the reaction mechanism was not affected [7].

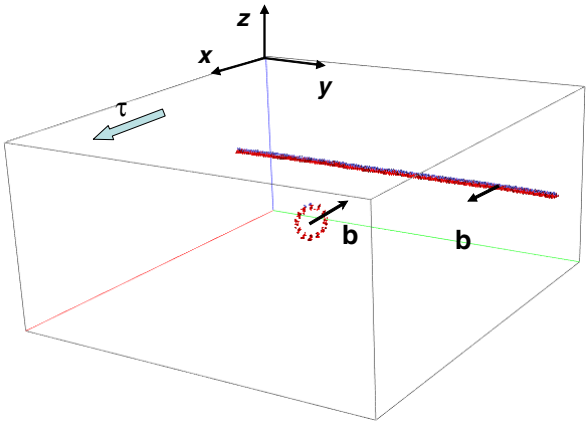

Figure 1. Schematic picture of the MD box containing the edge dislocation with $\boldsymbol{b} = \frac{1}{2}[111]$ and SIA dislocation loop with $\boldsymbol{b} = \frac{1}{2}[1\bar{1}1]$. The positive shear stress, τ, on the upper part of the box is shown by thick arrow. The coordinate axes x, y, z are oriented along $[111]$, $[\bar{1}\bar{1}2]$, $[1\bar{1}0]$, respectively.

The validity of MS and MD simulations depends on the robustness of the interatomic potential employed to calculate energy and forces. It is possible, therefore, that the dependence of the critical stress and mechanism on the temperature and loop size just described could be different with a different potential. Nearly all the work referred to above used the potential of Finnis–Sinclair type for iron obtained by Ackland *et al* [12]. As a result of more recent *ab initio* calculations, it is now known that it gives an inaccurate description of the single SIA and small SIA clusters [13], and of screw dislocation core structure [14]. A newer potential [15] fitted to *ab initio* data offers a better description of these defect properties. This potential does not describe directional bonding and magnetic effects, but is considered to be the best available for simulations involving millions of atoms. The model crystal is best considered as a bcc crystal with some iron-like properties at temperatures below the magnetic transformation. Since the breakaway mechanism and critical applied stress were found to be dependent on properties of SIA clusters and screw dipoles in the work referred to above, it is important to investigate dislocation–loop interaction with the newer potential. We apply it here in large-scale MD simulations performed on a crystal containing about three million atoms to study the interaction between an edge dislocation and a row of dislocation loops in the same orientation as in [7]. Each loop contains 169 SIAs, i.e. is of 4 nm size, which is intermediate between the sizes considered in [7]. The effects of both temperature and applied strain rate have been considered.

2. Simulation technique

The simulation model developed by Osetsky and Bacon [16] and applied in [7, 8] was employed. The principal axes x, y and z of the simulated body centred cubic crystal were oriented along the $[111]$, $[\bar{1}\bar{1}2]$ and $[1\bar{1}0]$ directions, respectively. The initially straight edge dislocation with slip plane x–y was created along the y direction and had Burgers vector $\boldsymbol{b} = \frac{1}{2}[111]$ parallel to the x axis (see figure 1). Periodic boundary conditions were applied along the x and y directions. The box was divided into three parts along z. The upper and lower parts consisted of several atomic planes in which atoms were rigidly fixed in their original position, whereas atoms in the inner region were free to move in the MD cycles. A glide

force on the dislocation was generated by the relative displacement of the rigid blocks in the x direction, which corresponds to simple shear strain e_{xz}. The corresponding resolved shear stress induced by the applied deformation was calculated as $\tau = F_x/A_{xy}$, where F_x is the total force in the x direction on the lower outer block from all atoms in the inner region and A_{xy} is the xy cross-section area of the box.

To allow for the possibility of the dislocation becoming elongated in the x direction at the critical stress, τ_c, as observed in earlier works [6, 11], the size of the inner region of the MD box was chosen to be 179×3, 59×6 and 49×2 atomic planes along x, y and z, respectively. Thus, the box volume was $45 \times 41 \times 20$ nm^3 and contained about 3.1 M mobile atoms. Earlier work [16] has shown that boundary effects are not significant for models of this size. An interstitial dislocation loop of hexagonal shape with sides along $\langle 112 \rangle$ directions and containing 169 interstitial atoms was placed initially with its centre about 3 nm below the dislocation line, as shown in figure 1. Its Burgers vector was $\frac{1}{2}[1\bar{1}1]$. (A loop with $\boldsymbol{b} = \frac{1}{2}[\bar{1}11]$ would react with the dislocation line in the same way by symmetry.) Identification of the position and structure of the dislocation core and loop during simulation was realized by using atomic disregistry analysis [16] and/or by identifying atoms with coordination number less than eight [17] and having high potential energy.

The interatomic potential for bcc Fe developed by Ackland *et al* [15] was used. The integration of Newton's equations was performed using a velocity Verlet scheme at constant time step equal to 5 fs. All calculations were done in the framework of a microcanonical NVE ensemble, where particle number, system volume and total energy are conserved if the work of external forces is taken into account. No additional temperature control was applied, for the temperature increase over the simulation time was negligible: the maximum was approximately 2 K, observed in modelling at 1 K for an accumulated strain of 2%. Temperature, T, and applied strain rate, $\dot{\varepsilon}$, were varied from 1 to 600 K and 10^6 to 5×10^7 s^{-1} (equivalent to steady state dislocation velocity 3.6–180 m s^{-1}), respectively. The physical time and number of MD time steps for completing a reaction between the dislocation and loop depended on $\dot{\varepsilon}$ and T. The fastest reaction occurred over 0.25 ns of MD time at the highest strain rate and temperature, while the longest reaction lasted more than 5 ns.

The results are presented in two sections. In the first, section 3.1, the reaction at the lowest T and $\dot{\varepsilon}$ is considered in detail, with attention paid to the atomic-level mechanisms involved in the reaction. A comparison of the results obtained for different strain rates and temperatures is presented in the second section, section 3.2, followed by discussion and conclusions.

3. Results

3.1. Mechanism of interaction at 1 K

The stress–strain curve for the dislocation–loop reaction simulated with $\dot{\varepsilon} = 10^6$ s^{-1} at 1 K is presented in figure 2. It is seen that the reaction proceeds in a series of steps, as indicated on the figure. They are described in the following and the corresponding dislocation–loop configurations are presented by the visualization snapshots in figure 3.

Step 1–Step 2. The initially straight dislocation starts to glide (to the right in figure 3) when applied strain is about 0.08% and τ reaches 60 MPa. When this happens, the SIA loop glides towards the dislocation slip plane under the mutual attraction between the two defects and the uppermost segment of it coalesces with the dislocation to form a segment with Burgers vector $\boldsymbol{b} = [010]$ through the reaction

$$\tfrac{1}{2}[111] + \tfrac{1}{2}[\bar{1}1\bar{1}] = [010]. \tag{1}$$

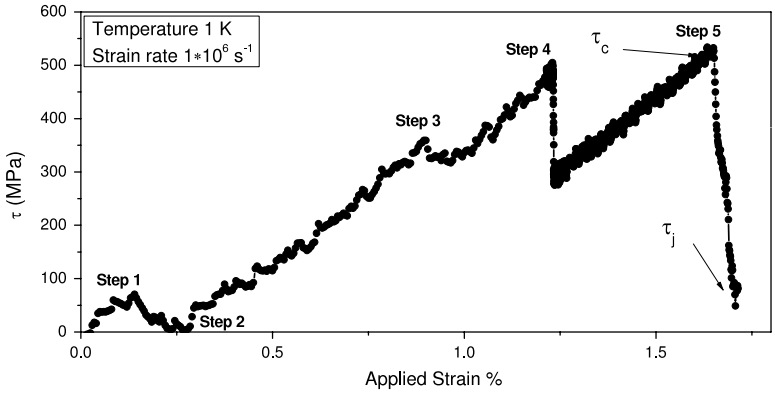

Figure 2. Stress–strain curve for dislocation–loop interaction at $T = 1$ K and $\dot{\varepsilon} = 10^6$ s^{-1}.

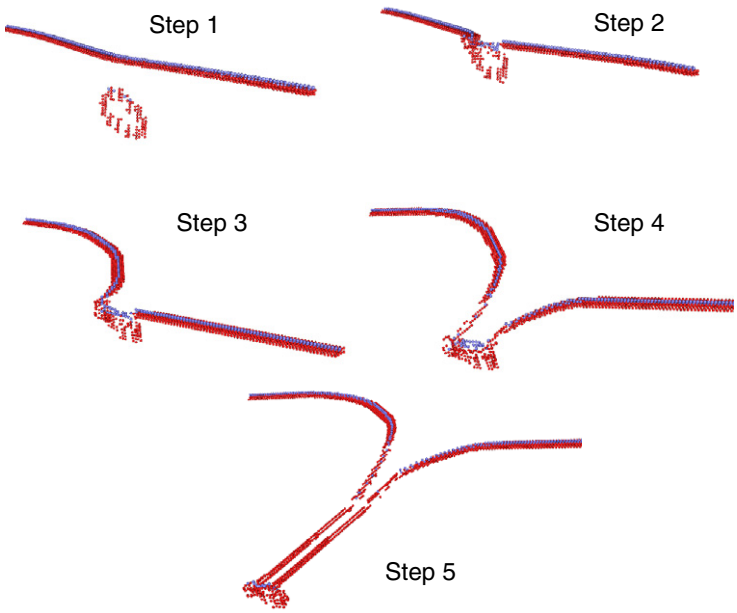

Figure 3. Visualizations of the dislocation and loop during their interaction at $T = 1$ K and $\dot{\varepsilon} = 10^6$ s^{-1}. The frames correspond to the steps marked on the plot of figure 2.

This energetically favourable coalescence is as predicted by Frank's b^2 rule for dislocation reactions.

Step 2–Step 3. The dislocation is pinned by the loop because the [010] segment is not glissile in the $(1\bar{1}0)$ glide plane of the dislocation. The stress increases with increasing strain as the dislocation bows between the periodic loops in the simulation. Serrations in the stress–strain plot correspond to the glide of kinks nucleated where the dislocation joins the loop.

Step 3–Step 4. The dislocation continues to bow between the loops and when τ reaches 500 MPa at step 4, the arms of the dislocation adjacent to the [010] segment are pulled

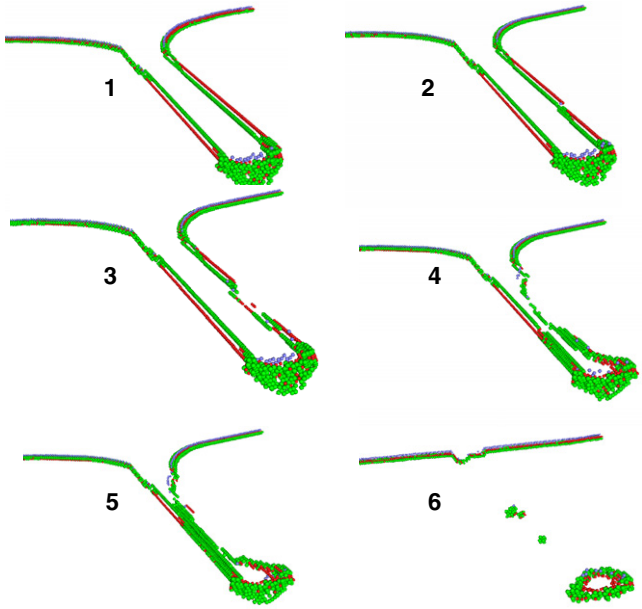

Figure 4. Visualization of the interaction just before and after release of the dislocation from the loop at $T = 1$ K and $\dot{\varepsilon} = 10^6$ s^{-1}.

into screw orientation. The formation of a screw dipole allows the non-screw segments of dislocation connected with each other through the periodic boundaries to propagate further and the stress falls to about 300 MPa.

Step 4–Step 5. The non-screw parts of the dislocation glide forward under increasing stress and the length of screw segments increases. At the same time, the [010] segment starts to glide downwards across the loop on a (101) plane and when the applied stress reaches the maximum value, τ_c, of 530 MPa, one screw segment moves towards the other by cross-slip and they annihilate, thereby releasing the dislocation from the loop. The nucleation of double kinks on the screws that give rise to this cross-slip occurs well away from the loop and [010] segment. The loop is reformed with $\boldsymbol{b} = \frac{1}{2}[1\bar{1}1]$, but with fewer SIAs than before the reaction. A few SIAs are left where the screws were first annihilated and the remainder are absorbed by the dislocation in the form of a double superjog. The unpinned, jogged dislocation glides away under a stress, τ_j, of 60 MPa.

The mechanism involved in the stages leading to the final release of the dislocation from the loop is revealed in more detail in the visualization snapshots presented in figure 4, which start in frame 1 when the dipole length reaches about $100b$, and figure 5, which shows the jogged dislocation in greater detail looking along the [111] slip direction after it has been released from the loop. In frame 1 of figure 4, the screw side-arms have already cross-slipped from the $(1\bar{1}0)$ plane. It is not clear why cross-slip out of the plane of maximum applied resolved shear stress occurs, but it may be a result of glide of the [010] segment described above: the left and right screws in frame 1 have cross-slipped on the $(10\bar{1})$ and $(0\bar{1}1)$ planes, respectively, i.e. A–B and F–E in figure 5. In frame 2 a single kink (of size equal to one Peierls valley period) has nucleated on the screw on the left at its junction with the [010] segment. This reduces the separation of the two screws, i.e. their force of attraction is increased, and double kinks (again

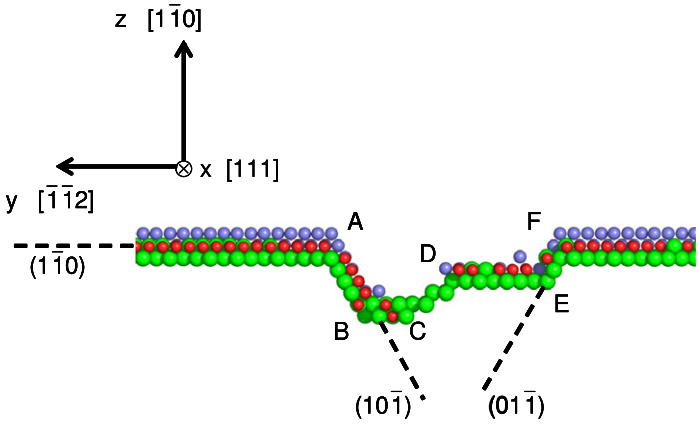

Figure 5. View along the [111] slip direction of the jogged dislocation in figure 4 after release from the loop.

of one Peierls period) are nucleated repeatedly near the centre of the right screw (see frames 3–5). This double-kink nucleation and glide causes the screw to cross back to the (1$\bar{1}$0) slip plane, i.e. E–D in figure 5. Note that only one of the dipole pair was involved in the slip process up to frame 5 and the reason for it is not clear. At this stage double kinks formed on both screws near their centres and annihilation started by cross-slip on the (1$\bar{2}$1) plane, i.e. B–C and D–C in figure 5. The critical stress, τ_c, and corresponding line shape are comparable with that for the Orowan mechanism, in which an edge dislocation overcomes an impenetrable particle by formation of screw segments as it wraps around the obstacle.

3.2. The effect of temperature and strain rate

The mechanism described above was also found in the simulations of dislocation–loop interaction at the same temperature of 1 K and the higher strain rates of 10^7 and 5×10^7 s^{-1}. The mechanism controlling the reaction at 300 and 600 K was observed to be different, however, for the SIA loop was completely absorbed at all three applied strain rates. A segment with $\boldsymbol{b} = [010]$ was again formed, but absorption of the loop was realized by glide of that segment across the loop, thereby converting its Burgers vector to $\frac{1}{2}$[111] and incorporating the loop in the dislocation as a superjog pair. It was found that the critical stress required for completion of the reaction depends on both temperature and applied strain rate. A comparison of the results obtained for the different simulation conditions is presented below.

Stress–strain curves for the reactions at the same strain rate, 10^6 s^{-1}, and three different temperatures, 1, 300 and 600 K, are presented in figure 6. The reactions at 300 and 600 K were essentially identical in nature so only that at 300 K is described in detail here. Visualizations showing the dislocation line and loop in [1$\bar{1}$0] and [111] projections during the simulation are presented in figures 7(a) and (b), respectively. Values of the applied shear stress at each stage are given against the [111] snapshots in figure 7(b). As can be seen in figure 6, glide of the edge dislocation starts at lower stress than at 1 K, i.e. 25–30 MPa compared with 60 MPa at 1 K. The loop slips to intersect the glide plane of the dislocation line, which is attracted towards it and moves forward (figure 7(a) frame 1), resulting in a negative value of the applied shear

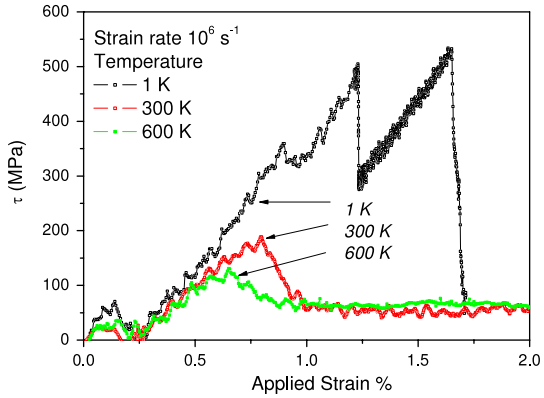

Figure 6. Stress–strain curve for dislocation–loop interaction at $\dot{\varepsilon} = 10^6\ \mathrm{s}^{-1}$ and $T = 1, 300$ or 600 K.

stress. As the applied strain increases further, the dislocation line reacts with the SIA loop to form a segment with $\boldsymbol{b} = [010]$, as in equation (1) (frame 2). As explained above, this segment is sessile in the $(1\bar{1}0)$ glide plane of the dislocation, which is forced to bow between the periodic row of loops as the applied strain is increased (frame 3). By frame 4, when the shear stress is 140 MPa, a dipole of two screw segments is formed at the loop and the [010] segment starts to slip across the loop in a (101) plane, a process assisted by cross-slip of the screw segments downwards on $(10\bar{1})$ planes (see the [111] projections in figure 7(b)). Glide of the [010] segment, combined with cross-slip of the screw side-arms, continues to a stress just above 180 MPa (frame 5), at which point $\boldsymbol{b}$ of the remaining part of the loop is converted to $\frac{1}{2}[111]$, thereby forming a superjog pair. The pair is pulled forward under the tension of the side-arms and so annihilates them (frame 6). The interstitial loop is totally absorbed on the dislocation by this reaction, which leaves a few vacancies behind, as can be seen in frame 6. Continued glide of the resulting edge dislocation with the superjog pair requires a stress of about 60 MPa.

The reaction at 600 K is the same as that at 300 K, although the critical stress is lower, namely 120 MPa compared with 180 MPa. It proceeds faster at both temperatures than at 1 K, which is believed to be due to higher mobility of the [010] edge and $\frac{1}{2}[111]$ screw segments when assisted by thermal vibrations.

Three important similarities among the reactions considered at high and low temperature can be noted. They are: (i) the formation of the $\langle 010 \rangle$ segment, which causes motion of the dislocation to cease; (ii) the maximum stress in the system occurs just before the motion of the screw segments occurs; (iii) partial or complete absorption of the pre-existing loop occurs in all reactions. Although the formation of the screw segments was common in all simulated reactions, their lengths were rather different. The length observed at 300 K was distinctly shorter than that for the reaction at 1 K, i.e. about $10b$ compared with $100b$, and even shorter screw segments were observed at 600 K.

No qualitative differences in the mechanism of interaction were found when different strain rates were applied, although increase in strain rate did result in increase in the critical stress. Values of the critical stress, τ_c, for all nine combinations of T and $\dot{\varepsilon}$ are plotted in figure 8(a). It is seen that τ_c depends strongly on T but only weakly on $\dot{\varepsilon}$ over the range considered. For example, τ_c decreases from 525 to 180 to 120 MPa as T is changed from 1 to 300 to 600 K at the lowest strain rate. The significant difference between 1 and 300 K arises from the differences in the reaction and breakaway mechanisms described above.

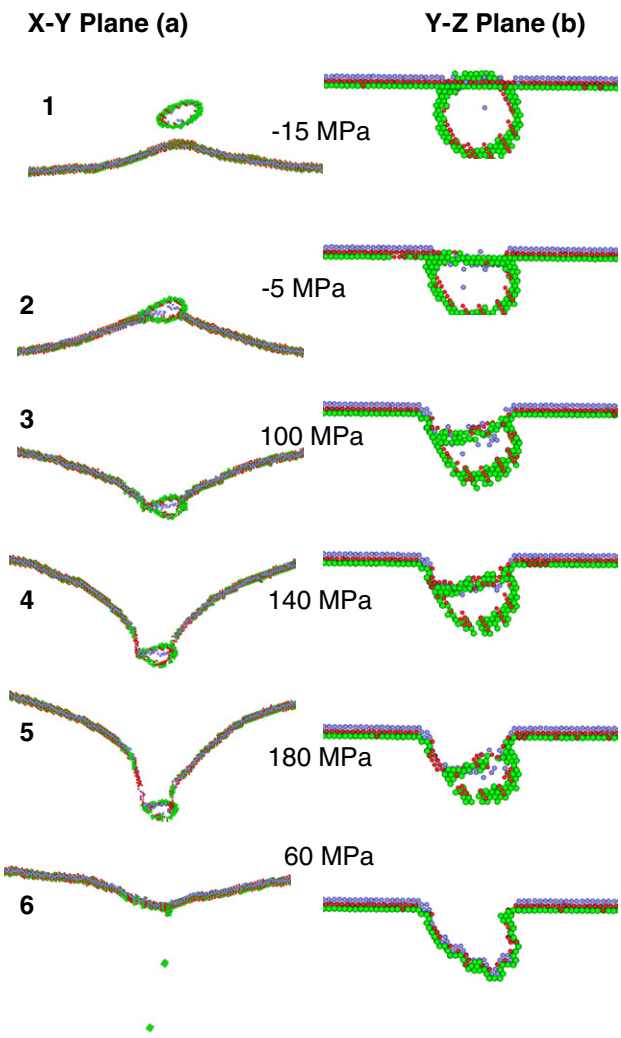

Figure 7. Visualizations showing the dislocation line and loop in (a) $[1\bar{1}0]$ and (b) [111] projection during the simulation of $T = 300$ K and $\dot{\varepsilon} = 10^6$ s^{-1}. Values of τ at each stage are given against the snapshots in (b).

Figure 8(b) includes the applied stress, τ_j, at which the jogged dislocation continues to glide after completion of the reaction with the loop. There is no difference between the 300 and 600 K data for the three applied strain rates. Interestingly, τ_j is the same for all three temperatures at $\dot{\varepsilon} = 10^6$ s^{-1} but the 1 K values show a strong dependence on applied strain rate, increasing from 60 to 100 MPa between $\dot{\varepsilon} = 10^6$ and 5×10^7 s^{-1}. The difference between 1 and 300 K cannot be attributed to a difference in the structure of the jogs, for τ_j plotted in figure 8(b) for 1 K corresponds to glide of the dislocation after reaction with the partially absorbed loop formed in the first reaction, i.e. the simulation was continued so that the dislocation passed through the crystal twice as a result of the periodicity along x. The loop was completely absorbed in the second reaction, thereby resulting in the same superjog structure as in reactions at the higher temperatures.

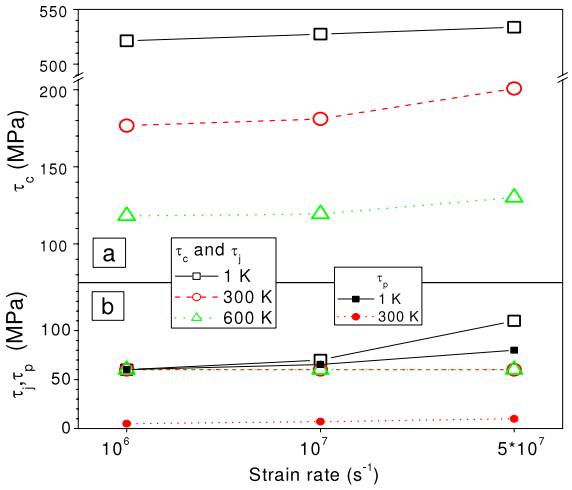

Figure 8. Values of (a) the critical stress, τ_c, and (b) the stress, τ_j, for continued glide of the jogged dislocation for all nine combinations of T and $\dot{\varepsilon}$ considered here. The stress, τ_p, for glide of a straight edge dislocation in a crystal free of other defects at $T = 1$ and 300 K is plotted in (b).

The applied stress, τ_p, at which the edge dislocation glides in a crystal free of other defects at 1 and 300 K is shown in figure 8(b). Only the τ_p values for 1 K show significant strain rate dependence and, interestingly, they are nearly the same as the corresponding τ_j values in figure 8(b). At 300 K, on the other hand, the unjogged dislocation moves under stress below 10 MPa, which is close to the level of uncertainty in the calculations, and the strain rate effect is negligible. The stress τ_p at this temperature is therefore almost an order of magnitude smaller than τ_j plotted in figure 8(b). It may be concluded that the effect of superjogs on the glide stress of an edge dislocation increases with increasing temperature.

4. Discussion

The effects revealed by the present work can be summarized as follows.

First, for the loop size considered, i.e. about 4 nm with 169 SIAs, neither the mechanism of reaction nor the critical stress, τ_c, depend strongly on the applied strain rate over the range considered ($10^6 \leqslant \dot{\varepsilon} \leqslant 5 \times 10^7$ s^{-1}). The only significant dependence on $\dot{\varepsilon}$ found was in the stress, τ_j, required for steady state glide of the jogged dislocation after the interaction at $T = 1$ K.

Second, a segment with $\boldsymbol{b} = [010]$ was observed to form by attractive reaction in all cases. This segment is sessile in the glide plane of the initial edge dislocation line and so raises the pinning force by restricting dislocation motion. When the dislocation breaks away, partial or complete absorption of the pre-existing loop occurs.

Third, the mechanisms that control τ_c are the same at 300 and 600 K, but different at 1 K. This results in large values of τ_c at low temperature. The controlling step at 1 K is cross-slip of one of the approximately 100b-long screw segments that are drawn out at high stress. This leads to pinching off of the screw dipole near its centre and reformation of part of the original $\frac{1}{2}[1\bar{1}1]$ loop. Only about one third of the SIAs are absorbed into the jogs formed on the dislocation. The creation of a screw dipole and subsequent pinching off at τ_c are the same as the critical condition for an edge dislocation to bypass an impenetrable obstacle by the Orowan

mechanism. At higher T, the controlling process appears to be either glide of the [010] segment across the loop or cross-slip of the screw side-arms, which are $<10b$ long, at their junction with the [010] segment. The two processes are inextricably linked and it is not possible to say which is the harder. Either way, the dipole simply disappears by rapid glide forward of the superjogs with $\boldsymbol{b} = \frac{1}{2}[111]$.

We now consider the results of two other simulation studies in the literature where the interaction between an edge dislocation and a periodic row of SIA loops in Fe was modelled with the same geometry as in the present work. Both used the many-body interatomic potential of Ackland *et al* [12], rather than the recent one used here [15].

Loops containing 99 SIAs were modelled in the work of Nomoto *et al* [6], with the dislocation induced to glide under the influence of a constant applied stress, rather than constant strain rate. The temperature was not given in the paper and the inter-loop spacing was smaller than the one used here, i.e. 35 nm compared with 41 nm. The final configuration after the dislocation had reacted with the loop was the same as that found here for the higher temperatures, namely glissile superjogs and a few vacancies. However, the transformation mechanism described was slightly different, for a [010] segment formed in the initial reaction; it appeared to split into two $\frac{1}{2}\langle 111\rangle$ segments that slipped down on the inclined (101) plane, e.g. $[010] = \frac{1}{2}[11\bar{1}] + \frac{1}{2}[\bar{1}11]$. As discussed in [7], the difference may be due to the mode of crystal loading, in which high applied stress resulted in high strain rate and high dislocation velocity. Furthermore, critical stress values were not obtained by the procedure used in [5]. Hence, it is not straightforward to compare the two sets of results.

The simulations of Bacon *et al* [7] treated 37-SIA and 339-SIA loops in models subjected to strain applied at a constant rate, which is the procedure adopted for the present study. The inter-loop spacing was the same as in this work. The results showed that small loops of 37 SIAs are easily absorbed as jogs on the dislocation because they spontaneously change their Burgers vector from $\frac{1}{2}[1\bar{1}1]$ to $\frac{1}{2}[111]$ on coming into contact with the dislocation. Independently of the strain rate, τ_c is small, i.e. between 13 and 27 MPa for 100 K $\leqslant T \leqslant$ 450 K. The critical process for large loops of 339 SIAs was found to be dependent on T but not on $\dot{\varepsilon}$. At 300 and 450 K the row of loops was overcome by the mechanism described here in section 3.2 for 300 and 600 K, i.e. formation of a [010] segment followed by its glide across the loop coupled with cross-slip of the screw side-arms under increasing stress, leading to formation of superjogs with $\boldsymbol{b} = \frac{1}{2}[111]$ and unzipping of the screw dipole by rapid glide of these jogs. As here, complete absorption of the loop occurred—see figure 5 of [7]. At $T = 100$ K, on the other hand, the [010] segment was observed to be immobile at 100 K and the dislocation broke away from the loop by cross-slip and mutual annihilation of its screw dipole side-arms—see figure 7 of [7]. This controlling process is the same as that found here for the 169-SIA loop at 1 K. The τ_c values for $\dot{\varepsilon} = 5 \times 10^6$ s^{-1} were 292, 212 and 165 MPa for $T = 100$, 300 and 450 K, respectively.

Comparison of these data from [7] with the τ_c values plotted in figure 8 for the simulations where the strain rate and temperature conditions were similar indicates that they are slightly lower, although the loop size was larger in the earlier study. They are sufficiently close, however, to suggest acceptable agreement between the mechanisms and results obtained with the older and much newer potentials. These potentials predict different equilibrium core structures for the screw dislocation and different preferred glide planes for this dislocation at low temperature [3, 14]. This is of interest for the present research because the critical stage for dislocation breakaway from large loops at low temperature is reached when the long segments of the screw dipole cross-slip and annihilate. It is not known whether the structure and Peierls stress of a dislocation segment with a $\langle 100\rangle$ Burgers vector is sufficiently different for the two potentials to affect this critical condition.

It is clear from the results reported here and those described in [6] and [7] that there is a transition in loop size between those small enough to experience easy rotation of their Burgers vector under the influence of interaction with an edge dislocation, and larger ones that are involved in a favourable reaction leading to formation of a segment with $\boldsymbol{b} = \langle 100 \rangle$, which is sessile in the dislocation glide plane. The former loops are relatively weak obstacles to dislocation glide. The latter are strong to an extent that depends on loop size and temperature, and possibly interatomic potential. Clearly, the mobility of both $\frac{1}{2}\langle 111 \rangle$ screws and $\langle 100 \rangle$ edge segments is important in determining the critical stress and the transitions in temperature and loop size that control the atomic mechanisms. An understanding of these issues is beyond the scope of the present work, and further research, involving extensive simulations, is required.

5. Conclusions

MD simulation has been used to investigate the influence of temperature, T, and strain rate, $\dot{\varepsilon}$, on the reaction between an edge dislocation line of the $\frac{1}{2}[111](1\bar{1}0)$ slip system and a periodic row of 169-SIA edge dislocation loops with $\boldsymbol{b} = \frac{1}{2}[1\bar{1}1]$ in a model of α-Fe based on the interatomic potential of Ackland *et al* [15]. The principal results are as follows.

(i) The reaction starts with coalescence of part of the line and loop to form an edge dislocation segment with $\boldsymbol{b} = [010]$. This segment is sessile in the $(1\bar{1}0)$ plane and so continued straining causes increasing applied stress, τ, as the line bows between the loops. Eventually, a dipole of screw segments attached to each [010] segment is formed, as described earlier in [6, 7]. Further evolution leading to breakaway of the line at critical stress τ_c depends on the temperature and involves one or a combination of the following processes.

(ii) At low T (1 K here) where thermal effects are negligible, a long ($\sim 100b$) screw dipole is drawn out and the controlling mechanism is annihilation of the dipole by screw cross-slip. It appears to be determined by the attractive mutual force between the screws, i.e. on their length and separation. This process is characterized by relatively high τ_c.

(iii) At high T (300 and 600 K here) the length of the screw dipole pinned at the loop is shorter ($<10b$) and the controlling mechanism is propagation by glide of the [010] segment over the loop surface under the applied stress τ, coupled with cross-slip of the short screws. This transforms the Burgers vector of the loop to that of the dislocation line, i.e. $\frac{1}{2}[111]$. The controlling process is temperature dependent and τ_c decreases with increasing T.

(iv) In general, τ_c increases with increasing $\dot{\varepsilon}$ strain rate and decreasing T. Over the ranges considered (10^6–5×10^7 s^{-1} and 1–600 K), the effect of temperature is much more important than that of strain rate.

(v) Interstitial atoms are absorbed onto the dislocation line by formation of superjogs under all the conditions studied. However, whereas the loop is completely absorbed in the process of glide of the [010] segment at 300 and 600 K, only about a fraction $\sim 1/3$ of the SIAs are absorbed at 1 K, where the line breaks away by pinching off of the screw dipole. The remainder of the interstitials in the latter case are left behind in a smaller version of the initial $\frac{1}{2}[1\bar{1}1]$ loop.

(vi) The applied shear stress for glide of the jogged dislocation is approximately the same as that for a straight edge dislocation at 1 K, but is higher by about an order of magnitude at 300 K.

(vii) The results here are consistent with those obtained previously for loops with either 37 or 339 SIAs in a model based on an older interatomic potential [12], except that the τ_c values are a little higher. Thus, a picture has emerged in which small loops are easily transformed

to $\boldsymbol{b} = \frac{1}{2}[111]$ type and are then absorbed at small τ_c at all temperatures; medium-to-large loops at 300 K and above are totally transformed to $\boldsymbol{b} = \frac{1}{2}[111]$ and are absorbed at higher τ_c by glide of a $\boldsymbol{b} = [010]$ segment; and medium-to-large loops at low T where thermal effects are negligible are only partly transformed to $\boldsymbol{b} = \frac{1}{2}[111]$ and so are only partially absorbed when the screw dipole pinches off at high τ_c.

Acknowledgments

This work was partially supported by the European Commission within the underlying Technology scheme of the European Fusion Programme. It was also partly supported by grant GR/S81162/01 from the UK Engineering and Physical Sciences Research Council; grant F160-CT-2003-508840 ('PERFECT') under programme EURATOM FP-6 of the European Commission; and partly by the Division of Materials Sciences and Engineering and the Office of Fusion Energy Sciences, US Department of Energy, under contract DE-AC05-00OR22725 with UT-Battelle, LLC.

References

[1] Ehrlich K 1999 *Phil. Trans. R. Soc. Lond.* A **357** 595
[2] Wirth B D, Caturla M J, Diaz de la Rubia T, Khraishi T and Zbib H 2001 *Nucl. Instrum. Methods Phys. Res.* B **180** 23
[3] Harry T and Bacon D J 2002 *Acta Mater.* **50** 209
[4] Osetsky Yu N, Bacon D J and Mohles V 2003 *Phil. Mag.* **83** 3623
[5] Bacon D J and Osetsky Yu N 2005 *Mater. Sci. Eng.* A **400/401** 353
Osetsky Yu N and Bacon D J 2005 *Mater. Sci. Eng.* A **400/401** 374
[6] Nomoto A, Soneda N, Takahashi A and Ishino S 2005 *Mater. Trans.* **46** 463
[7] Bacon D J, Osetsky Yu N and Rong Z 2007 *Phil. Mag.* **86** 3921
[8] Rong Z, Osetsky Yu N and Bacon D J 2005 *Phil. Mag.* **85** 1473
[9] Marian J, Wirth B D, Shäublin R, Odette G R and Perlado J M 2003 *J. Nucl. Mater.* **323** 181
[10] Jumel S, Van Duysen J C, Ruste J and Domain C 2005 *J. Nucl. Mater.* **346** 79
[11] Osetsky Yu N, Bacon D J, Serra A, Singh B N and Golubov S I 2000 *J. Nucl. Mater.* **276** 65
Terentyev D, Malerba L and Hou M 2007 *Phys. Rev.* B **75** 104108
[12] Ackland G J, Bacon D J, Calder A F and Harry T 1997 *Phil. Mag.* A **75** 713
[13] Willaime F, Fu C C, Marinica M C and Dalla Torre J 2005 *Nucl. Instrum. Methods Phys. Res.* B **228** 92
[14] Domain C and Monnet G 2005 *Phys. Rev. Lett.* **95** 215506
[15] Ackland G J, Mendelev M I, Srolovitz D J, Han D and Barashev A V 2004 *J. Phys.: Condens. Matter* **16** 1
[16] Osetsky Yu N and Bacon D J 2003 *Modelling Simul. Mater. Sci. Eng.* **11** 427
[17] Rodney D 2004 *Acta. Mater.* **52** 607